

A Digital Human Model for the Simulation of Dynamic Driving Maneuvers

Michael ROLLER^{a,1}, Vanessa DÖRLICH^a, Joachim LINN^a,
Staffan BJÖRKENSTAM^b and Peter MÅRDBERG^b

^a *Fraunhofer ITWM, Germany*

^b *Fraunhofer Chalmers Center, Sweden*

Abstract. In this work, a digital human model based on multibody system dynamics is used in a car pre-crash scenario. An optimal control approach is used to generate motion and control signals. The arms of the manikin are actuated by Hill muscles, while the rest of the body is controlled by joint torques. A full braking maneuver is investigated as an application case.

Keywords. Digital human model, Hill muscle, Optimal control, Dynamic driving, Pre-crash

1. Introduction

Digital human models (DHM) are widely used in automotive industry to simulate the driver in very early stages of product development, where no physical prototypes of the car exist. In case of crash simulation, detailed finite element (FE) models of the human body are used to simulate the highly dynamic impact and the resulting injuries in the human body [1,2,3]. Models with multibody system (MBS) kinematics are widely used when the reachability and the ergonomic assessment of the driver is investigated [4,5, 6,7]. These types of models are only used in static scenarios, where the car is standing or driving with constant velocity. In dynamic driving scenarios like cornering, sudden braking or pre-crash scenarios, neither FE nor MBS model types are applicable. Besides being difficult to control, FE models are too time consuming, as the simulated time span in dynamic driving is longer than in crash simulations. The kinematic models are not able to take into account dynamic loads and contact forces. Furthermore, the motion generation is difficult, because these models are usually based on forward or inverse kinematics.

2. Methods

In this work, we will present an approach for the enhancement of a multibody based DHM to generate human like motions for dynamic driving maneuvers. The human is

¹Corresponding Author: Michael Roller, Fraunhofer ITWM, Fraunhofer-Platz 1, 67663 Kaiserslautern, Germany; E-mail: michael.roller@itwm.fraunhofer.de

modelled as a multibody system for that purpose, where the limbs are rigid bodies, which are connected via joints. Hill muscles are used to implement digital versions of the real muscles in the human body and to actuate the multibody system. An optimal control algorithm, which is able to handle opening and closing of contacts, is developed in order to generate the dynamic human motion. It allows for the simulation of the dynamic interaction of the DHM with the car interior such as the seat, pedals or the steering wheel. In this approach, only some basic boundary conditions have to be described. These include the sitting posture of the human at starting time with two hands on the steering wheel and the trajectory of the car. Using a certain objective function, the optimal control approach then generates the desired control (muscle actuation) and the human motion. This approach has already been applied successfully to simulate dynamic motions of workers [8,9,10]. In this work we will show that it is also applicable in pre-crash scenarios, like full braking.

2.1. Biomechanical Multibody Model of the Human

The limbs of the human are modelled as rigid bodies with the mass and inertia tensor as physical properties. Their respective position and orientation in space are given by a translational vector and a rotation matrix. These rigid bodies are connected with rotational joints in a tree structure starting from the hip. In Figure 1, all degrees of freedom of the DHM are displayed. It is essentially the same manikin which was used in [9] to do a full body box lift. The degrees of freedom of each joint q control the position and

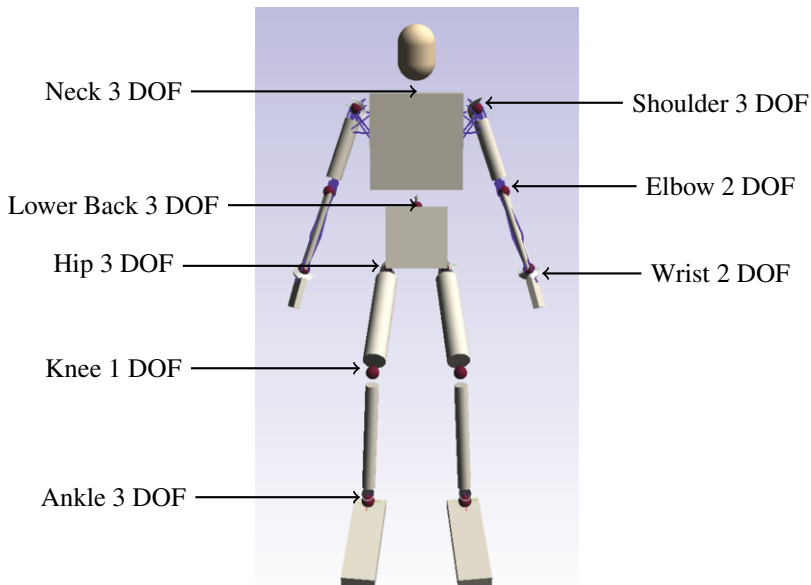


Figure 1. DHM with 40 degrees of freedom including the rigid body joint, which has 6 DOF

orientation of the corresponding child body in terms of the parent body, see [11] for more details. The hip is connected to the fixed world frame by a rigid body joint, which allows the DHM to translate and rotate freely in space. All of these degrees of freedom are col-

lected in the vector $\mathbf{q} = (q_1, \dots, q_N)$, which describes the position and orientation of each body and therefore the state of the multibody system.

A digital version of the human muscles is used to actuate the multibody model representing the human skeleton. As in [12,13], muscles of simple Hill-type are utilized. The rheological model of the muscle consists of a contractile element (CC) and an elastic spring (PEC), which are connected in parallel. The force generated by the CC depends

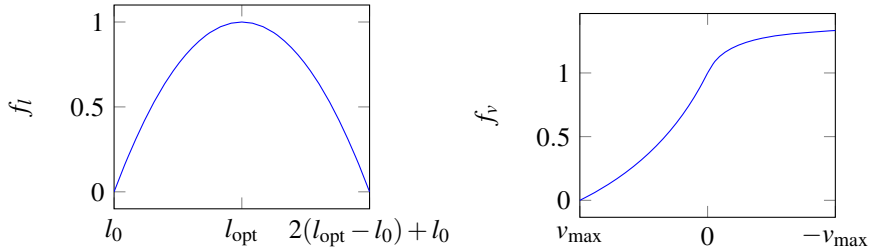


Figure 2. Left: Force-length relation of CC-element. Right: Force-velocity relation of CC-element, where $v > 0$ corresponds to an eccentric and $v < 0$ to a concentric motion.

on the current length l , the contraction velocity \dot{l} , the actuation level $u \in [0, 1]$ and the maximum isometric force F_{max} of the muscle and is given by

$$F_{CC} = f_l(l)f_v(\dot{l})uF_{max} . \tag{1}$$

The force-length and the force-velocity dependencies are visualized in Figure 2. Here, l_0 represents the minimum and l_{opt} the optimal muscle length. The negative scalar $v_{max} < 0$ is the maximal contractive velocity of the muscle.

The PEC element is modelled using a linear elastic spring $F_{PE} = k(l - l_0)$ with stiffness $k \in \mathbb{R}_+$. Since the elements are connected in parallel, the muscle force is a linear superposition of both,

$$F_m = F_{CC} + F_{PE} = f_l(l)f_v(v)uF_{max} + k(l - l_0) . \tag{2}$$

In order to use the rheological Hill elements in a MBS, a piecewise linear string is used to represent the muscle path. This string is defined by $M \geq 2$ points \mathbf{x}_i , where each point is positioned on the surface of a rigid body. The length of the muscle is calculated by summarizing the distances between points. With these quantities and an activation u , the scalar muscle force $F_m \in \mathbb{R}$ is calculated using equation (2). Then, a force pointing in the direction of neighbouring points with magnitude F_m is applied in every point \mathbf{x}_i , which induces a force and torque on the corresponding body.

In this work, both arms are actuated by Hill muscles. Each arm consists of the same 27 muscles which were used in [10] to control the seven degrees of freedom of the arm. In Figure 3, all digital muscles of the right arm are visualized in detail. The remaining joints of the human are controlled by joint torques, which are the ankles, knees, hips and neck.

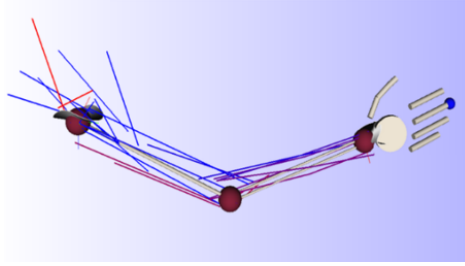


Figure 3. Multibody model of the arm including 27 muscles.

2.2. Discrete Mechanics and Optimal Control with Constraints

Traditionally, human simulation tools use quasi-static poses to emulate motion, which severely limits the possible set of producible motions. For pre-crash simulations, we want to be able to realistically simulate highly dynamic motions, where modelling of inertia effects becomes relevant. To that end, we model the manikin as a dynamical system and use optimal control methods to compute the motions. This approach was already used for the simulation of different working tasks [8,9,10,14].

An optimal control problem is defined abstractly by the following formulas

$$\min_{\mathbf{q}, \mathbf{u}} J = \int_{t_0}^{t_f} \phi(\mathbf{q}, \dot{\mathbf{q}}, \mathbf{u}, \dot{\mathbf{u}}) dt \quad (3)$$

s.t.

$$\frac{\partial L}{\partial \mathbf{q}}(\mathbf{q}, \dot{\mathbf{q}}) - \frac{d}{dt} \frac{\partial L}{\partial \dot{\mathbf{q}}}(\mathbf{q}, \dot{\mathbf{q}}) + \mathbf{F}(\mathbf{q}, \dot{\mathbf{q}}, \mathbf{u}) + \mathbf{G}^T(\mathbf{q})\lambda = 0, \quad (4)$$

$$\mathbf{g}(\mathbf{q}) = 0, \quad (5)$$

$$\mathbf{h}(\mathbf{q}|_{t_0}, \mathbf{q}|_{t_f}, \dot{\mathbf{q}}|_{t_0}, \dot{\mathbf{q}}|_{t_f}, t_0, t_f) = 0, \quad (6)$$

$$\mathbf{c}^- \leq \mathbf{c}(\mathbf{q}, \mathbf{u}, \lambda) \leq \mathbf{c}^+. \quad (7)$$

As already introduced in Section 2.1, the variable \mathbf{q} represents the temporal trajectory of the MBS between the starting time t_0 and the end time t_f . The control signals for the muscles and the joint torques are combined in the variable \mathbf{u} . In (3), the objective function J is introduced, where ϕ is a measure for the state of the system. As a side constraint, the constrained Euler Lagrange equations (4)-(5) have to be fulfilled, where the function L represents the Lagrangian of the system, the function \mathbf{g} summarises the constraints and the variable λ is the corresponding Lagrangian multiplier. A general formulation of the boundary conditions is given by (6) with the function \mathbf{h} . Additional equality and inequality constraints can be included in the optimal control problem by (7). Here \mathbf{c}^- is the lower and \mathbf{c}^+ is the upper bound of the constraint function \mathbf{c} . This is a general description of many different constraints like box constraints on the controls, constancy of a function or path constraints. Altogether, the optimal control problem is an optimization problem and the solutions are temporal trajectories of the MBS \mathbf{q} , the control signals \mathbf{u} and the Lagrangian multiplier λ .

In order to solve the optimal control problem, the continuous problem (3)-(7) is discretised into a non-linear programming problem using discrete mechanics, see [15,16] for more details. This approach is called DMOCC (discrete mechanics and optimal control with constraints). The discrete equations of motions derived in this way have been shown to be superior compared to standard discretisations since they preserve characteristics of the continuous system such as conservation of momentum and a good energy behaviour. This results in very stable integrators, which in practice allows us to use large time steps when solving our problems. The resulting non-linear programming problem is solved with the interior point method [17].

3. Simulation Results of a Sudden Braking Maneuver

As application case we investigate the dynamic scenario of full braking of a car with the DHM as the driver. The car is modelled as a plate, where two pedals, a seat and a steering wheel are rigidly mounted. This sledge is mounted using a one dimensional translation joint on the fixed root frame. The car model is visualized in Figure 4.

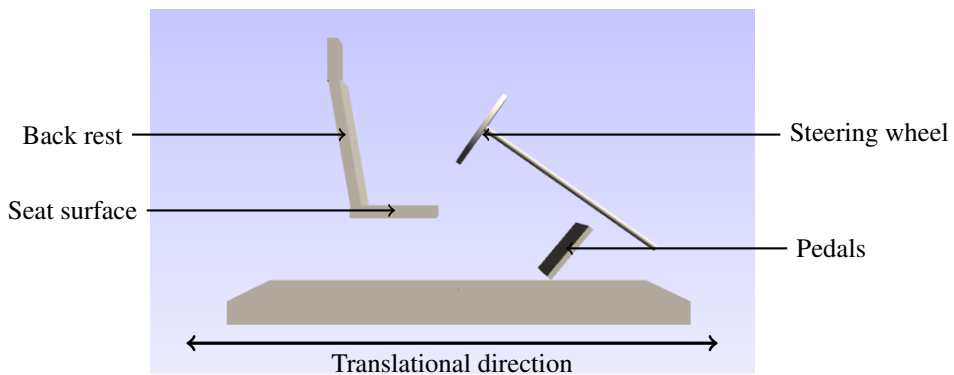


Figure 4. Simplified model of a car used in the simulation.

The manikin specified in Section 2.1 is seated into the simplified car model as follows. Both feet are rigidly mounted on the pedals in an arbitrary position, but fixed over the time span of the simulation, which means that the position on the pedals is a free variable in the optimal control problem. Also the constraint forces are restricted, such that Coulomb's law of static friction holds. The buttocks of the human are connected in the same way to the lower seat surface. Both hands are connected rigidly to the steering wheel in a fixed position and orientation. In case of the hands, the constraint forces are not restricted, such that the constraint force realizes grabbing the wheel with a closed hand. For more details on how this is technically implemented we refer to [10].

The simulation is split in two connected phases. In the first phase the car is accelerated to 5 m/s from starting at standstill. The manikin is constrained to an arbitrary but fixed position during the whole phase. This is done to avoid a dynamic preparation for the sudden deceleration of the manikin by moving the upper body against the direction of driving, which would be unnatural behaviour. The duration of the phase is fixed, because a constant force is used to accelerate the car. It has to be noted, that due to the choice

of special time stepping algorithm, it is sufficient to discretise this phase by only one interval. This reduces the number of variables and therefore decreases the computation time.

At the beginning of the second phase the slide stops immediately to 0 m/s , which is done by adding an additional dynamic constraint, see [10,18]. Therefore, the kinetic energy of the car is completely absorbed by a phase specific constraint force. At the end of the phase, the manikin is forced to be at rest as well. The DHM has to use the muscle and control torques to eliminate the kinetic energy during the phase as there are no additional constraint forces. The duration of this phase is free, which means that it is an additional variable of the optimization problem. Minimal control is used as objective function for this application case, which means that in objective function (3) $\phi = \mathbf{u} \cdot \mathbf{u}$ is used.

In Figure 5, the movement of the manikin during the second phase is visualized in a series of pictures. The simulation starts at the top left corner at picture (a) and time is moving through the rows to the right. At the end of the row the simulation continues at the left side of the next row. It can be observed that the upper body of the manikin is moving towards the steering wheel at the beginning of the simulation, see picture (b). This is caused by a lack of strength of the muscles in the arms and the control torques in the lower back to eliminate the remaining kinetic energy immediately. After some time, this movement stops and the body is moving in direction of the back rest until it is at rest, see picture (c).

4. Discussion

It has to be noted that the motion was generated by the DMOCC method with only the constraints described in section 3. Thus, no time demanding forward kinematic positioning of the manikin has to be performed. Additionally, all specified muscle forces and actuation signals are computed by this method as a by-product, which could be used in a further physiological evaluation. The computation time for such a model on a modern personal computer is in the range of minutes. Therefore, it is possible to do many different variations using this simulation approach, e.g. in the positioning of the seat, the position of the steering wheel or the velocity of the car as well as different posture, anthropometry and weight of the driver.

In this work, we have shown that an optimal control approach including muscles as actuators can be used to create a realistic motion of a manikin in a pre-crash simulation. The simulation times of such a model are in the range of minutes, which is much faster than detailed FE simulations. These FE models usually run for hours without having any active control of the DHM. We observed that in this type of optimal control simulation of a DHM in a dynamic pre-crash scenario, the computational model anticipates the sudden perturbation and prepares dynamically in an unnatural manner for it. In this work, this behaviour was suppressed by fixing the degrees of freedom of the DHM during the first phase. However, this can also be used as a method to determine physically optimal behaviour of a human in dynamic scenarios using a suitable formulation of the optimal control problem.

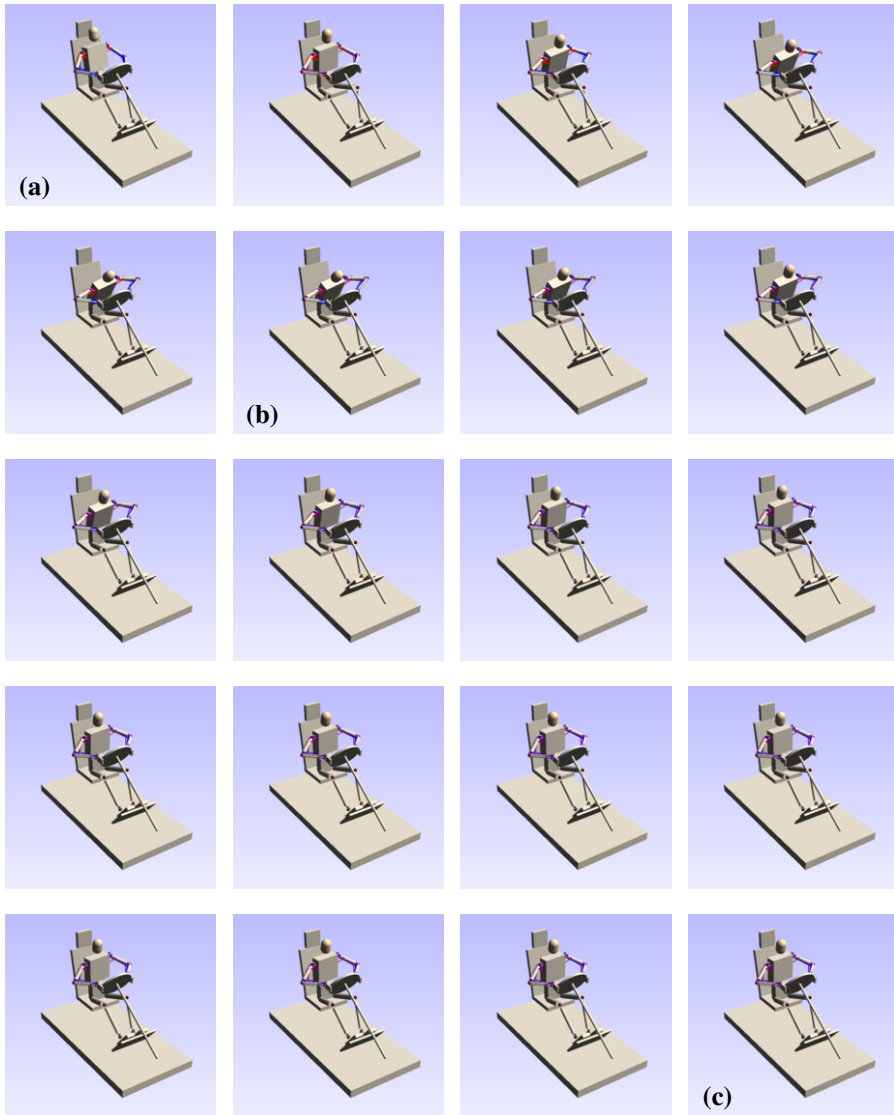


Figure 5. Screenshots at different time stamps of the DHM during the second phase. The time is running from left to right through the rows and from top to bottom.

References

- [1] Iwamoto M, Kisanuki Y, Watanabe I, Furusu K, Miki K, Hasegawa J. Development of a finite element model of the total human model for safety (THUMS) and application to injury reconstruction. In: Proceedings of the international IRCOBI Conference; 2002. .
- [2] Forman JL, Kent RW, Mroz K, Pipkorn B, Bostrom O, Segui-Gomez M. Predicting rib fracture risk with whole-body finite element models: development and preliminary evaluation of a probabilistic analytical framework. In: Annals of Advances in Automotive Medicine/Annual Scientific Conference. vol. 56. Association for the Advancement of Automotive Medicine; 2012. p. 109.
- [3] Östh J, Mendoza-Vazquez M, Linder A, Svensson MY, Brodin K. The VIVA OpenHBM finite element 50th percentile female occupant model: whole body model development and kinematic validation. In: IRCOBI Conference; 2017. p. 13–15.
- [4] van der Meulen P, Seidl A. Ramsis—the leading cad tool for ergonomic analysis of vehicles. In: International Conference on Digital Human Modeling. Springer; 2007. p. 1008–1017.
- [5] Blanchonette P. Jack human modelling tool: A review. DEFENCE SCIENCE AND TECHNOLOGY ORGANISATION VICTORIA (AUSTRALIA); 2010.
- [6] Hanson L, Högberg D, Carlson JS, Delfs N, Brodin E, Mårdberg P, et al. Industrial Path Solutions—Intelligently Moving Manikins. In: DHM and Posturography. Elsevier; 2019. p. 115–124.
- [7] Högberg D, Hanson L, Bohlin R, Carlson JS. Creating and shaping the DHM tool IMMA for ergonomic product and production design. International Journal of the Digital Human. 2016;1(2):132–152.
- [8] Björkenstam S, Nyström J, Carlson JS, Roller M, Linn J, Hanson L, et al. A framework for motion planning of digital humans using discrete mechanics and optimal control. In: 5th International Digital Human Modeling Symposium, Bonn Germany, June 26-28, 2017. Federal Institute for Occupational Safety and Health; 2017. p. 64–71.
- [9] Björkenstam S, Leyendecker S, Linn J, Carlson JS, Lennartson B. Inverse Dynamics for Discrete Geometric Mechanics of Multibody Systems With Application to Direct Optimal Control. Journal of Computational and Nonlinear Dynamics. 2018;13(10):101001.
- [10] Roller M, Björkenstam S, Linn J, Leyendecker S. Optimal control of a biomechanical multibody model for the dynamic simulation of working tasks. In: Proceeding of the 8th ECCOMAS Thematic Conference on Multibody Dynamics; 2017. .
- [11] Featherstone R. Rigid body dynamics algorithms. Springer; 2014.
- [12] Maas R, Leyendecker S. Optimal control of biomechanical motion using physiologically motivated cost functions. In: The 2nd joint international conference on multibody system dynamics; 2012. .
- [13] Maas R, Leyendecker S. Biomechanical optimal control of human arm motion. Proceedings of the Institution of Mechanical Engineers, Part K: Journal of Multi-body Dynamics. 2013;227(4):375–389.
- [14] Obentheuer M, Roller M, Björkenstam S, Berns K, Linn J. Comparison of Measured EMG Data with Simulated Muscle Actuations of a Biomechanical Human Arm Model in an Optimal Control Framework—Direct Vs. Muscle Synergy Actuation. In: IFToMM World Congress on Mechanism and Machine Science. Springer; 2019. p. 26–33.
- [15] Marsden JE, West M. Discrete mechanics and variational integrators. Acta Numerica. 2001;10:357–514.
- [16] Leyendecker S, Ober-Blöbaum S, Marsden JE, Ortiz M. Discrete mechanics and optimal control for constrained systems. Optimal Control Applications and Methods. 2010;31(6):505–528.
- [17] Wächter A, Biegler LT. On the implementation of an interior-point filter line-search algorithm for large-scale nonlinear programming. Mathematical programming. 2006;106(1):25–57.
- [18] Koch M, Leyendecker S. Structure preserving optimal control of a three-dimensional upright gait. In: Multibody Dynamics. Springer; 2016. p. 115–146.